Bypassing Orthogonal Relaying Transmissions via Spatial Signal Separation

Diomidis S. Michalopoulos, *Member, IEEE,* and George K. Karagiannidis, *Senior Member, IEEE*

***Abstract*—We argue for incorporating Space Division Multiple Access (SDMA) into cooperative relaying, in order to bypass orthogonal relaying transmissions and thus achieve diversity gain without any cost on the available degrees of freedom. In particular, we propose a cooperative relaying scheme that utilizes two single-antenna relays and multiple antennas at the destination terminal, in order to spatially separate the concurrently arriving signals. The whole concept is based upon two key elements: a) To combat the half-duplex constraint by having two relays transmitting alternatively, i.e., the one receiving while the other transmitting and vice versa, and b) to spatially separate the signals arriving concurrently at the destination using the well-known optimum combining technique. Closed-form expressions for the average capacity and outage probability are provided. Numerical results manifest that the proposed model outperforms orthogonal relaying as well as distributed space-time coding in terms of average capacity and outage probability, owing to the former's advantage of higher spectral efficiency.**

***Index Terms*—Space division multiple access (SDMA), optimum combining, wireless relaying technology.**

I. Introduction

RECEIVING from multiple antennas is a well-known method that attains the beneficial effects of diversity and thus provides higher quality of service in wireless communication systems. Despite its ability to combat small-scale fading, however, the above technique is unable to tackle the problem of hidden terminals, where high large-scale attenuation on the channel between the transmitter and the receiver, caused by either shadowing or path-loss, significantly degrades the performance. Cooperative relaying [1]-[11] on the other hand has been recently proposed as a promising method that offers robustness against this problem, by employing a number of relaying terminals that are willing to forward the information received by the source terminal to a specified destination one. In this way, the multiple paths through which communication is achieved are spatially separated from one another, reducing thus their level of correlation. This leads to spatial-diversity achievement, resulting finally in better error performance [6]-[11].

Paper approved by F. Santucci, the Editor for Wireless System Performance of the IEEE Communications Society. Manuscript received January 31, 2009; revised October 7, 2009 and February 16, 2010.

This work was presented partially at the International Conference on Communications (ICC08).

D. S. Michalopoulos is with the Department of Electrical and Computer Engineering, The University of British Columbia, Vancouver, BC V6T 1Z4, Canada (e-mail: dio@ece.ubc.ca).

G. K. Karagiannidis is with the Department of Electrical and Computer Engineering, Aristotle University of Thessaloniki, GR-54124 Thessaloniki, Greece (e-mail: geokarag@auth.gr).

Digital Object Identifier 10.1109/TCOMM.2010.080310.090066

A. Motivation

Nonetheless, as demonstrated in many papers dealing with cooperative diversity, the advantages of the above protocols come at a spectral efficiency cost. This is mainly because of

- the half-duplex constraint (i.e., the fact that the relays cannot transmit and receive simultaneously and at the same frequency band [1]), resulting in "two-stage" transmissions from the source terminals to the destination ones
- the fact that the multiple relays must transmit in orthogonal channels in either the time or the frequency domain, in order for the destination to be able to separate the multiple relaying transmissions thus taking full advantage of the multiple available paths.

Therefore, particularly for the case of multiple participating relays per source-destination pair, one may realize that according to conventional orthogonal relaying protocols the available degrees of freedom are not fully exploited, since there exists a resource waste on account of the orthogonality among the multiple relaying transmissions. As a result, the overall capacity per unit bandwidth is considerably reduced, a fact which has negative impact on the outage performance as well [3]-[5].

Furthermore, this drawback of spectral inefficiency becomes more evident in cases where the destination terminal is capable of employing multiple receiving antennas (for example, in the uplink of cellular communications or wireless LANs), since for those cases one may argue that the extra degrees of freedom induced by this multiple-antenna usage may be utilized for achieving higher multiplexing gains, instead of diversity ones. To the best of the authors' knowledge, although there exist some remarkable works in the literature where protocols that mitigate the spectral efficiency loss are proposed [12]-[14], none of them takes advantage of the extra resource that multiple-antenna reception entails, leaving thus the potential for spatial signal separation unexploited.

B. Contribution

To this end, in this paper we propose utilizing the extra degrees of freedom that the employment of multiple receiving antennas at the destination entails, towards the incorporation of Space Division Multiple Access (SDMA) in cooperative relaying systems. In particular, a novel relaying protocol that utilizes two single-antenna relays and multiple antennas at the destination is proposed, which bypasses orthogonal relaying transmissions and thus combats the aforementioned spectral inefficiency disadvantage. Specifically, the multiple antennas are used so as to spatially separate the concurrently arriving

signals and thus let the source and the relays transmit in the same band at the same time, while still being able to attain diversity.

The whole concept is based on two key ideas: a) To combat the half-duplex constraint by having the two relays transmitting alternatively, i.e., as long as the one operates at the transmitting mode the other remains at the receiving mode and vice versa, and b) to spatially separate the signals arriving concurrently at the destination (i.e., one directly from the source and one from one of the relays) using the well-known SDMA technique [15, Ch. 14]-[16, Ch. 10]. As a result, this enables cooperative communications to provide diversity and/or robustness against large-scale fading without paying the price of spectral inefficiency that described above.

Additionally, we provide an analysis of the distribution of the resulting signal-to-interference-plus-noise ratio (SINR), that allows us to derive approximate closed-form expressions for the average capacity per unit bandwidth, as well as outage probability. The numerical outage results are also verified by simulations.

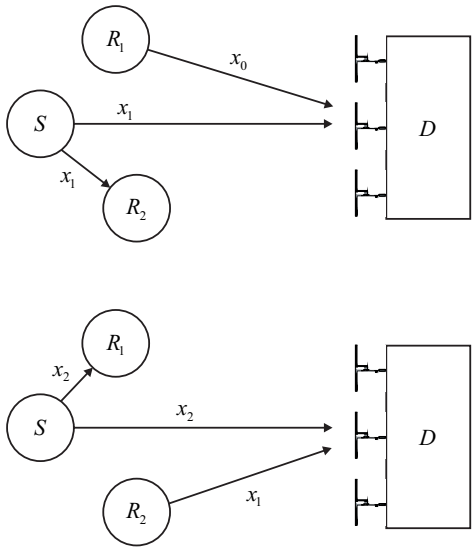

Fig. 1. The proposed protocol: first and second subframe.

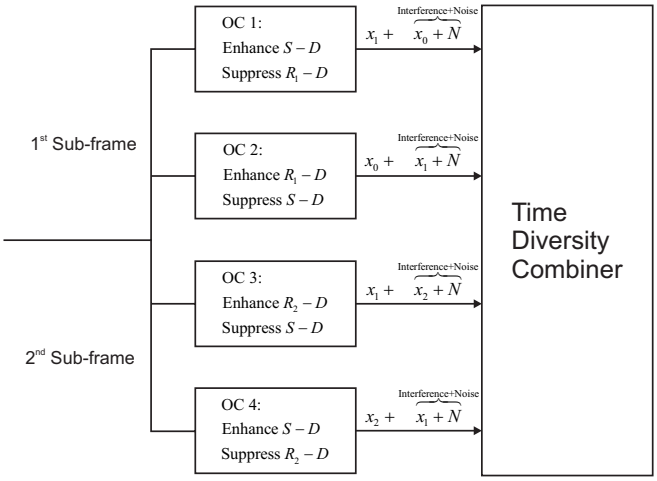

Fig. 2. The proposed protocol: first and second combining stage.

II. System Model

We consider a single-antenna source node S, communicating with an L-antenna destination node, denoted by D. Two single antenna relays, namely R_1 and R_2, are willing to assist this communication, by decoding the message received from S and forward the re-encoded data to D, operating thus in the well-known decode and forward (DF) mode. In order to protect the system from error propagations, the relays are assumed to decode only if the signal-to-noise-ratio (SNR) at their inputs is greater than a pre-specified activation threshold value, denoted by T, following thus the so-called threshold DF protocol (see e.g., [17]). It is further assumed that the value of T is appropriately selected so that practically zero error propagations take place; that is, the signal transmitted by the relays is assumed error-free. Moreover, half-duplex relaying is assumed, implying that the relays cannot transmit and receive simultaneously, but on different timeslots. The whole system is operating in flat, Rayleigh fading environment, that is supposed to be slowly varying. The AWGN noise powers in each receiving antenna are identical with one another, denoted by σ^2.

A. Protocol Description

Contrary to typical multi-relay cooperative diversity systems, the relays in the proposed scheme are assumed not to decode at the same time, nor to transmit the same symbol to the destination in orthogonal channels. Instead, they are activated alternatively, according to the protocol shown in Fig. 1. In particular, the whole transmission period is divided into a series of frames, each one consisting of two subframes: During the first subframe, R_1 transmits to the destination what it previously received, while R_2 listens to the source; during the second subframe, the roles of R_1 and R_2 are inverted, i.e., R_2 transmits while R_1 listens.

Let us assume that the symbols x_1 and x_2 are transmitted by the source at the first and second subframe, respectively. The received signal at the destination at these subframes consists of the signal received directly from the source and the signal received from one of the relays, that was actually received by the corresponding relay one subframe earlier. Hence, denoting by $\mathbf{r}_i$ the L-dimensional vector received at the destination at the ith subframe, we have

$$\mathbf{r}_1 = x_1\mathbf{u}_{SD} + x_0\mathbf{u}_{R_1D} + \mathbf{n}_1 \tag{1}$$

$$\mathbf{r}_2 = x_2\mathbf{u}_{SD} + x_1\mathbf{u}_{R_2D} + \mathbf{n}_2. \tag{2}$$

In (1) and (2), the column vectors $\mathbf{u}_{SD}$ and $\mathbf{u}_{R_iD}$ $(j, i = 1, 2)$ are mutually independent L-dimensional zero-mean complex Gaussian random vectors that represent the spatial signatures of the S-D and the R_i-D channel, respectively; $\mathbf{n}_j$ $(j = 1, 2)$ is the noise vector at the jth subframe. The mean powers of the components of $\mathbf{u}_{SD}$ are identical with each other, denoted by Ω_{SD}; likewise, $\Omega_{R_1D} = \Omega_{R_2D} = \Omega_{RD}$ are the mean powers of the components of $\mathbf{u}_{R_1D}$ and $\mathbf{u}_{R_2D}$, implying independent and identically distributed (i.i.d.) fading between the relays and the destination. For the sake of simplicity of the analysis, unitary source and relay transmitting powers are assumed; the analysis however can be easily extended to the

case of non-identical transmitting powers between the source and the relays, as well as non-identically distributed fading on the R_1-D and R_2-D channels.

It is important to note that the transmissions of the source and the relays require the usage of a single channel (i.e., they occur concurrently and at the same frequency band). This implies that *the proposed scheme offers no loss in spectral efficiency compared to conventional point-to-point communications*, while still achieving diversity since two independent replicas of each symbol are received by D. This is contrary to what is usually assumed in the literature, where the beneficial effects of diversity come at the expense of spectral efficiency loss, since at most half of the available degrees of freedom are utilized [1], [3].

B. System Model Variations: Deployment of Infrastructure-Based or Mobile Relays

Depending on the type of the relaying terminals employed, i.e., infrastructure based relays or mobile relays, two variations of the main concept are introduced, dubbed here as variations 1 and 2, respectively. In fact, variation 1 corresponds to the case where the relays are "isolated" from one another; variation 2 to the case where some inter-relay communication exists. Below, these variations are described in detail.

1) Variation 1: Infrastructure-based relays: Observing Fig. 1, one may note that according to the proposed setup, along with the signal transmitted by the source the receiving relay may receive part of the signal incident from the transmitting relay. Apparently, the presence of this inter-relay link impedes the decoding of the signal incident from the source and actually represents an interfering component to the S-R channel. However, for the particular case of fixed, infrastructure-based relays, such interference may be canceled using highly directive antennas at the relays, hence eliminating inter-relay communications. Then, the decision regarding the activation of the receiving relay at the ensuing subframe is based upon comparing the SNR of the corresponding S-R channel with the activation threshold, T.

2) Variation 2: Mobile relays: On the other hand, for the versatile case where the relays are generally non-fixed and employ non-directive antennas, each of them is assumed to perform single-antenna interference cancelation mechanisms in order to cancel out the signal received from the other relay. In particular, the relays employ the so-called mono interference cancelation (MIC) algorithm proposed in [18]. This algorithm consists of multiplying the received complex signal (which equals the complex sum of the signal vectors received from the source and the transmitting relay, together with the noise component) with a unitary vector on the direction of the complex conjugate vector of the interferer; then taking the imaginary part of the resulting product leads to completely canceling out the interfering signal. However, the power of the desired-signal component undergoes an attenuation since only a part of its total power is projected to the imaginary axis.

The above procedure results in an output instantaneous SNR having the form of [18, eq. (6)]

$$SNR_{MIC} = \frac{\mathrm{Im}^2\left\{h_I^* h_D\right\}}{|h_I|^2}\frac{1}{\sigma^2} \tag{3}$$

where the nominator of the second term of (3) is unity because of the assumption that both the source and the relays transmit with unitary power; h_D, h_I denote the instantaneous complex channel gain corresponding to the desired and the interfering signal, respectively. If, for instance, R_1 operates at the receiving mode, while R_2 at the transmitting mode at a given time instance t, then h_D represents the complex channel gain between S and R_1; h_I is the complex channel gain between R_2 and R_1. One may note from (3) that the instantaneous SNR after applying the MIC algorithm equals the SNR of the desired signal, though attenuated by a factor of $\mathrm{Im}^2\left\{h_I^* h_D\right\} / |h_I|^2$. Hence, its upper and lower bounds are given by

$$0 \le SNR_{MIC} \le |h_D|^2 \frac{1}{\sigma^2} \tag{4}$$

implying that in the best case the output SNR equals that of the infrastructure-based relay case, where the interference is canceled without reducing the power of the desired signal; in the worst case, the desired signal is eliminated together with the interfering one. In other words, employing the MIC algorithm as described above (and presented in detail in [18]) results in completely canceling out inter-relay interference, yet with some power cost. This cost on the output SNR at the relays and thereby on the overall performance is quantified in Section V. It should be noted that, apparently, the decision on whether a mobile relay is activated (according to the threshold-DF protocol) is determined by the result of comparing SNR_{MIC} with T. Next, we derive the distribution of the overall SINR, i.e. the SINR at the output of the destination terminal.

III. On the Overall Instantaneous SINR

A. First Combining Stage: Signal Separation through SDMA

As observed from (1) and (2), in each subframe the destination receives two co-channel signals, one incident from the source and another from either R_1 or R_2. Taking advantage of the multiple antennas at the destination, these two signals are separated with one another by utilizing the well-known concept of SDMA. In particular, in each subframe the combined signal received by the multiple antennas passes through two space diversity combiners, that weight each of the L diversity branches by a complex weight. These weights are appropriately chosen so that the two combiners perform the so-called *optimum combining* [19], that leads to the maximum SINR in wireless systems in the presence of co-channel interference and thermal noise. For example, during the first subframe the first optimum combiner (OC1) considers the S-D signal as the desired one, and the R_1-D as the interfering, whereas the second combiner (OC2) considers these signals as the interference and the desired one, respectively. During the second subframe, the two combiners involved (namely OC3 and OC4) extract the S-D signal out of the "interfering" R_2-D one, and the R_2-D out of the "interfering" S-D signal, respectively. Fig. 2 summarizes the way these combiners are

allocated in each subframe, as well as the resulting signals at their outputs.

Let us adopt the general notation of A representing the terminal transmitting the desired signal, and B representing the interfering one, with $A, B \in \{S, R_1, R_2\}$ (e.g., during the first subframe $A = S,\ B = R_1$). Define

$$\gamma_{AD} \triangleq \mathbf{u}_{AD}^H \mathbf{u}_{AD}/\sigma^2 \tag{5}$$

i.e., γ_{AD} represents the instantaneous SNR of the A-D link at the output of the combiner given that no interference takes place. This is the case when the relay supposed to transmit at a given subframe (e.g., R_1 referring to the first subframe) is inactive due to the previously mentioned thresholding mechanism, i.e., the source-relay SNR at the previous subframe was below the threshold T. Moreover, we denote by $\overline{\gamma}_{AD} = \Omega_{AD}/\sigma^2$ the average SNR per antenna associated with the A-D link. Due to the fact that $\mathbf{u}_{AD}$ is comprised of L complex Gaussian components, γ_{AD} is an L-order Gamma distributed random variable (RV); its probability density function (PDF) is thus given by

$$f_{\gamma_{AD}}(\gamma_{AD}) = \frac{\gamma_{AD}^{L-1}}{\overline{\gamma}_{AD}^{L}\Gamma(L)} \exp\left(-\frac{\gamma_{AD}}{\overline{\gamma}_{AD}}\right) \tag{6}$$

where $\Gamma(\cdot)$ is the gamma function defined in [20, eq. (8.310.1)].

Because of the slow fading assumption, constant spatial signatures in each subframe are considered. Therefore, the $L \times L$-dimensional interference-plus-noise covariance matrices are constructed as

$$\mathbf{\Phi}_B = \mathbf{u}_{BD}\mathbf{u}_{BD}^H + \sigma^2 \mathbf{I}_L \tag{7}$$

where $\mathbf{I}_L$ is the L-dimensional identity matrix and $(\cdot)^H$ represents the Hermitian operator. Let $\mathbf{w}_{A,B}$ represent the complex weight vectors associated with the combiner that filters the A-D and nulls the B-D channel. With optimum combining, $\mathbf{w}_{A,B}$ are given as [19]

$$\mathbf{w}_{A,B} = \mathbf{\Phi}_B^{-1}\mathbf{u}_{AD}.$$

Consequently, denoting with P_A and P_{B+N} the signal power at the output of the combiner associated with the signal incident from A, and the signal-plus-noise power associated with terminal B, respectively, the resulting SINR is given by [19], [21]

$$\begin{aligned}\gamma_b^{A,B} &= \frac{P_A}{P_{B+N}} = \frac{\left|\mathbf{w}_{A,B}^H \mathbf{u}_{AD}\right|^2}{\mathbf{w}_{A,B}^H \mathbf{\Phi}_B \mathbf{w}_{A,B}} \\ &= \frac{\left(\mathbf{u}_{AD}^H \mathbf{\Phi}_B^{-1}\mathbf{u}_{AD}\right)^2}{\mathbf{u}_{AD}^H \mathbf{\Phi}_B^{-1}\mathbf{u}_{AD}} = \mathbf{u}_{AD}^H \mathbf{\Phi}_B^{-1}\mathbf{u}_{AD}.\end{aligned} \tag{8}$$

B. Second Combining Stage: Time Diversity

As observed from Figs. 1 and 2, the destination collects two independent replicas of each of the transmitting symbols within a window of two consecutive subframes. Hence, the attained diversity order can be increased if the signals issuing from the first combining stage are combined again into a proper time-diversity combiner. Next, the operation of this second-stage combiner that maximizes the overall SINR is analyzed.

Without loss of generality, we focus henceforth on the reception of x_1. The resulting analysis thus refers to the performance associated with that symbol, and actually represents the overall performance due to the symmetry assumption between the S-R_1-D and S-R_2-D links. Symbol x_1 is extracted once at the first subframe from S, with a suppressed version of that transmitted on R_1-D being the interference; it is also extracted at the second subframe from R_2, where the S-D link is interfering. Hence, the instantaneous signal powers at output of the first-stage combiners associated with these two versions of x_1 are taken from (8) as

$$P_S^{(x_1)} = \left(\mathbf{u}_{SD}^H \mathbf{\Phi}_{R_1}^{-1}\mathbf{u}_{SD}\right)^2,\ P_{R_2}^{(x_1)} = \left(\mathbf{u}_{R_2D}^H \mathbf{\Phi}_S^{-1}\mathbf{u}_{R_2D}\right)^2$$

whereas the corresponding interference-plus-noise powers as

$$P_{R_1+N}^{(x_0)} = \mathbf{u}_{SD}^H \mathbf{\Phi}_{R_1}^{-1}\mathbf{u}_{SD},\ P_{S+N}^{(x_2)} = \mathbf{u}_{R_2D}^H \mathbf{\Phi}_S^{-1}\mathbf{u}_{R_2D}.$$

The two versions of x_1 together with the interference components are co-phased and added into the second-stage time diversity coherent equal gain combiner (EGC). The resulting overall SINR, namely γ, is the ratio of the total signal power over the total interference plus noise power, i.e.,

$$\begin{aligned}\gamma &= \frac{\left(\sqrt{P_S^{(x_1)}} + \sqrt{P_{R_2}^{(x_1)}}\right)^2}{P_{R_1+N}^{(x_0)} + P_{S+N}^{(x_2)}} \\ &= \mathbf{u}_{SD}^H \mathbf{\Phi}_{R_1}^{-1}\mathbf{u}_{SD} + \mathbf{u}_{R_2D}^H \mathbf{\Phi}_S^{-1}\mathbf{u}_{R_2D} \\ &= \gamma_b^{S,R_1} + \gamma_b^{R_2,S}\end{aligned} \tag{9}$$

Notice that γ is the sum of SINRs in the first and second subframe; this means that the performance of the second-stage EGC is identical with that of a maximal ratio combiner (MRC). This can be also verified by noting that the weights of a MRC in this particular case would be identical, namely $\omega_1 = \sqrt{P_S^{(x_1)}}/P_{R_1+N}^{(x_0)} = \sqrt{P_{R_2}^{(x_1)}}/P_{S+N}^{(x_2)} = \omega_2 = 1$[1]. The reader should also note that the overall SINR expression shown in (9) is general enough so as to also hold for the case where one of the relays is inactive due the aforementioned thresholding mechanism. Should R_1 be inactive, for example, then the corresponding interference-plus-noise covariance matrix becomes $\mathbf{\Phi}_{R_1} = \sigma^2 \mathbf{I}_L$, yielding $\gamma_b^{S,R_1} = \mathbf{u}_{SD}^H \mathbf{u}_{SD}/\sigma^2 = \gamma_{SD}$; should R_2 be inactive, then the time-diversity EGC does not take the second subframe into account, hence $\gamma_b^{R_2,S} = 0$.

IV. Variation 1: Overall SINR Distribution

A. Moment Generating Function (MGF) Analysis

The MGF of γ is defined as

$$\mathcal{M}_\gamma(s) = E_\gamma\left\langle e^{-s\gamma}\right\rangle = \sum_{i=1}^{4} \rho_i E_\gamma\left\langle \exp\left(-s\gamma\,|\Theta_i\right)\right\rangle \tag{10}$$

where $E_X\langle\cdot\rangle$ denotes expectation over the random variable X; $\Theta_1, ..., \Theta_4$ are the four cases that may be considered, corresponding to each of the possible combinations of whether

[1]We note that a second-stage MRC in our case would differ from the conventional one used in noise limited systems in the sense that the denominator in our case is the instantaneous interference plus noise power, whereas in conventional systems is the average noise power; the resulting SINRs, however, are the same.

or not R_1 and R_2 are active; $\rho_1, ..., \rho_4$ are the corresponding occurrence probabilities. The above cases are further analyzed below.

1) Case Θ_1, Both R_1 and R_2 active: Should this be the case, the received signal at both subframes contains the symbol x_1 together with an interference component. Under the i.i.d. Rayleigh fading assumption on S-R_1 and S-R_2, this case occurs with probability

$$\rho_1 = \Pr\{\gamma_{SR_1}, \gamma_{SR_2} > T\} = e^{-\frac{2T}{\overline{\gamma}_{SR}}}. \quad (11)$$

Let us keep the notation of A representing the desired and B the interfering terminal. The eigen decomposition of the covariance matrix $\mathbf{\Phi}_B$ in (7) yields

$$\mathbf{\Phi}_B = \mathbf{V}_B \mathbf{\Lambda}_B \mathbf{V}_B^H \quad (12)$$

where $\mathbf{V}_B$ is the eigenvector matrix and $\mathbf{\Lambda}_B = \text{diag}\left(\lambda_1^B, ..., \lambda_L^B\right)$, with λ_i^B representing the ith eigenvalue of $\mathbf{\Phi}_B$, which can be easily evaluated as

$$\lambda_i^B = \begin{cases} \mathbf{u}_{BD}^H \mathbf{u}_{BD} + \sigma^2, & i = 1 \\ \sigma^2, & i = 2, ..., L \end{cases}. \quad (13)$$

Therefore, combining (10), (8) and (12) we obtain the MGF of $\gamma_b^{A,B}$ as

$$\mathcal{M}_{\gamma_b^{A,B}}(s) = E_{v_{A_i} v_{A_i}^*} \left\langle \exp\left(-\sum_{i=1}^{L} \frac{s v_{A_i} v_{A_i}^*}{\lambda_i^B} \right) \right\rangle \quad (14)$$

where $(\cdot)^*$ stands for the complex conjugate of its argument and v_{A_i} is the ith component of the vector $\mathbf{v}_{AD} = \mathbf{V}_B \mathbf{u}_{AD}$. Note that the Hermitian nature of $\mathbf{\Phi}_B$ implies that the latter transformation is unitary, hence $E\langle v_{A_i} v_{A_i}^* \rangle = \Omega_{AD}$. Consequently, averaging over the exponential distribution of $v_{A_i} v_{A_i}^*$ and then using (13), (5) and (14), we may obtain the conditional MGF of $\gamma_b^{A,B}$ given γ_{BD} as [22]

$$\mathcal{M}_{\gamma_b^{A,B}}(s|\gamma_{BD}) = \prod_{i=1}^{L} \frac{\lambda_i^B}{\lambda_i^B + s\Omega_{AD}} = \frac{(\gamma_{BD}+1)/\overline{\gamma}_{AD}}{(\gamma_{BD}+1)/\overline{\gamma}_{AD} + s} \left(\frac{1/\overline{\gamma}_{AD}}{1/\overline{\gamma}_{AD} + s} \right)^{L-1}. \quad (15)$$

Then, $\mathcal{M}_{\gamma_b^{A,B}}(s)$ is obtained by averaging (15) over the PDF given in (6), which using [20, eq. (3.353.5)], [20, eq. (8.352.3)] and [23, eq. (6.5.9)] yields

$$\mathcal{M}_{\gamma_b^{A,B}}(s) = \int_0^\infty \mathcal{M}_{\gamma_b^{A,B}}(s|\gamma_{BD}) f_{\gamma_{BD}}(\gamma_{BD}) d\gamma_{BD} = \frac{\left[\mathcal{E}_L\left(\frac{1+s\overline{\gamma}_{AD}}{\overline{\gamma}_{BD}} \right) + L\overline{\gamma}_{BD} \mathcal{E}_{L+1}\left(\frac{1+s\overline{\gamma}_{AD}}{\overline{\gamma}_{BD}} \right) \right] e^{\frac{1+s\overline{\gamma}_{AD}}{\overline{\gamma}_{BD}}}}{\overline{\gamma}_{BD}(1+s\overline{\gamma}_{AD})^{L-1}} \quad (16)$$

where $\mathcal{E}_n(\cdot)$ is the exponential integral function of order n, defined in [23, eq. (5.1.4)]. It follows then from (9) that the overall MGF for this case is $\mathcal{M}_\gamma(s|\Theta_1) = \mathcal{M}_{\gamma_b^{S,R}}(s) \mathcal{M}_{\gamma_b^{R,S}}(s)$, where due to symmetry it holds $\overline{\gamma}_{R_1 D} = \overline{\gamma}_{R_2 D} = \overline{\gamma}_{RD}$.

2) Case Θ_2, R_1 active; R_2 inactive: The occurrence probability for this case is evaluated as

$$\rho_2 = e^{-\frac{T}{\overline{\gamma}_{SR}}} \left(1 - e^{-\frac{T}{\overline{\gamma}_{SR}}} \right) = e^{-\frac{T}{\overline{\gamma}_{SR}}} - e^{-\frac{2T}{\overline{\gamma}_{SR}}}. \quad (17)$$

The overall SINR is $\gamma = \gamma_b^{S,R_1}$, hence the resulting MGF $\mathcal{M}_\gamma(s|\Theta_2)$ is that given in (16), with $A = S, B = R_1$.

3) Case Θ_3, R_1 inactive; R_2 active: Because of the symmetry between the S-R_1 and S-R_2 links, it holds $\rho_3 = \rho_2$. Due to the absence of interference at the first subframe, the SINR now becomes $\gamma = \gamma_{SD} + \gamma_b^{R_2,S}$. The MGF of γ for this case is therefore derived as

$$\mathcal{M}_\gamma(s|\Theta_3) = \mathcal{M}_{\gamma_{SD}}(s) \mathcal{M}_{\gamma_b^{R_2,S}}(s) = \frac{\mathcal{M}_{\gamma_b^{R_2,S}}(s)}{(1+s\overline{\gamma}_{SD})^L} \quad (18)$$

where $\mathcal{M}_{\gamma_{SD}}(s) = (1+s\overline{\gamma}_{SD})^{-L}$, obtained by averaging $\exp(-s\gamma_{SD})$ over the PDF of γ_{SD} given in (6).

4) Case Θ_4: Both R_1 and R_2 inactive: This case occurs with probability $\rho_4 = \left(1 - e^{-\frac{T}{\overline{\gamma}_{SR}}}\right)^2$. Since the SINR now reduces to $\gamma = \gamma_{SD}$, the resulting MGF for Θ_4 is $\mathcal{M}_\gamma(s|\Theta_4) = \mathcal{M}_{\gamma_{SD}}(s) = (1+s\overline{\gamma}_{SD})^{-L}$.

Considering the above, the MGF of the overall SINR, $\mathcal{M}_\gamma(s)$, can be expressed as

$$\mathcal{M}_\gamma(s) = \rho_1 \mathcal{M}_{\gamma_b^{S,R}}(s) \mathcal{M}_{\gamma_b^{R,S}}(s) + \rho_2 \mathcal{M}_{\gamma_b^{S,R}}(s) + \rho_3 (1+s\overline{\gamma}_{SD})^{-L} \mathcal{M}_{\gamma_b^{R,S}}(s) + \rho_4 (1+s\overline{\gamma}_{SD})^{-L} \quad (19)$$

where $\mathcal{M}_{\gamma_b^{S,R}}(s)$, $\mathcal{M}_{\gamma_b^{R,S}}(s)$ are taken from (16).

B. An Approximate MGF Expression

The above analysis provides an exact closed-form expression for the overall MGF, by substituting in (10) the conditional MGF expressions, conditioned on the cases $\Theta_1, ..., \Theta_4$. Nevertheless, an approximate yet much easier to process closed-form expression for $\mathcal{M}_{\gamma_b^{A,B}}(s)$ (and thus for $\mathcal{M}_\gamma(s)$) can be derived, by using a first-order Taylor approximation on the conditional MGF $\mathcal{M}_{\gamma_b^{A,B}}(s|\gamma_{BD})$ [24, ch. 7], from which $\mathcal{M}_{\gamma_b^{A,B}}(s)$ is derived in terms of $E_{\gamma_{BD}}\langle \gamma_{BD} \rangle = L\overline{\gamma}_{BD}$ as

$$\mathcal{M}_{\gamma_b^{A,B}}(s) \simeq \frac{(L\overline{\gamma}_{BD}+1)/\overline{\gamma}_{AD}}{(L\overline{\gamma}_{BD}+1)/\overline{\gamma}_{AD} + s} \left(\frac{1/\overline{\gamma}_{AD}}{1/\overline{\gamma}_{AD} + s} \right)^{L-1}. \quad (20)$$

It turns out that this approximation on the MGF of optimum combining SINR is accurate in most cases, as it also noted in [25]. Consequently, a tight approximate expression on the overall MGF is directly derived from (19), where the $\mathcal{M}_{\gamma_b^{S,R}}(s)$, $\mathcal{M}_{\gamma_b^{R,S}}(s)$ are now taken from (20), instead of (16).

C. PDF of γ

An approximation of the PDF of γ, $f_\gamma(\cdot)$, is derived by taking the inverse Laplace transform of the approximate MGF of γ yielding

$$f_\gamma(x) \simeq \rho_1 \left[\Xi_1 e^{-\frac{(L\overline{\gamma}_{RD}+1)x}{\overline{\gamma}_{SD}}} + \sum_{i=2}^{L} \frac{\Xi_i x^{i-2} e^{-\frac{x}{\overline{\gamma}_{SD}}}}{(i-2)!} + \Psi_1 e^{-\frac{(L\overline{\gamma}_{SD}+1)x}{\overline{\gamma}_{RD}}} + \sum_{i=2}^{L} \frac{\Psi_i x^{i-2} e^{-\frac{x}{\overline{\gamma}_{RD}}}}{(i-2)!} \right] + \rho_2 \left[\Delta_1 e^{-\frac{(L\overline{\gamma}_{RD}+1)x}{\overline{\gamma}_{SD}}} + \sum_{i=2}^{L} \frac{\Delta_i x^{i-2} e^{-\frac{x}{\overline{\gamma}_{SD}}}}{(i-2)!} \right] + \rho_3 \left[F_1 e^{-\frac{(L\overline{\gamma}_{SD}+1)x}{\overline{\gamma}_{RD}}} + \sum_{i=2}^{L} \frac{F_i x^{i-2} e^{-\frac{x}{\overline{\gamma}_{RD}}}}{(i-2)!} \right]$$

$$+\sum_{i=1}^{L}\frac{\Upsilon_i x^{i-1}}{(i-1)!}e^{-\frac{x}{\overline{\gamma}_{SD}}}\Bigg]+\rho_4\frac{x^{L-1}e^{-\frac{x}{\overline{\gamma}_{SD}}}}{\overline{\gamma}_{SD}^{L}\,(L-1)!} \tag{21}$$

where Ξ_i, Ψ_i, Δ_i, $\digamma_i$, Υ_i, $i=1,...,L$ are the fraction nominators derived by expanding the MGF in partial fractions, as it is shown in Appendix A.

V. Variation 2: Overall SINR Distribution

Recall that variation 2 refers to the case where communication between the relays exists; the inter-relay signal is suppressed using the so-called MIC algorithm proposed in [18] and analyzed in Section II-B2. In fact, utilizing the MIC algorithm leads to completely canceling out the inter-relay signal, however the value of the source-relay SNR is decreased. Consequently, given the assumption that the value of the activation threshold, T, is appropriately selected so as the signals forwarded by the relays are error-free, the SINR analysis for variation II is the same as that of variation I shown in Section IV, yet the occurrence probabilities of the cases $\Theta_1,...,\Theta_4$ are now different. These probabilities are derived in the following subsection.

A. Derivation of the Occurrence Probabilities, $\rho_1,...,\rho_4$

Variation 2 implies that the decision on whether the relays are activated is determined by the comparing the SNR of the MIC algorithm with T. Hence, in order to obtain the occurrence probabilities $\rho_1,...,\rho_4$ it suffices to derive the CDF of the SNR_{MIC} expression given in (3). Following similar analysis as in [26], we may express SNR_{MIC} as a fraction of the inner product of h_I^* and $h_D e^{j\pi/2}$ divided by σ^2, yielding

$$\begin{aligned}SNR_{MIC}&=\frac{1}{\sigma^2}\frac{|h_I^*|^2\,|h_D|^2\sin^2\theta}{|h_I|^2}\\&=\gamma_{SR}\sin^2\theta\end{aligned} \tag{22}$$

where θ denotes the absolute difference in the argument of the desired and the interfering signal at the receiving relay, which is uniformly distributed in $(-\pi,\pi]$; e.g., when the desired symbol is x_1, $\theta=|\arg(h_{SR_2})-\arg(h_{R_1R_2})|$ with h_{AB} denoting the complex channel gain between terminals A and B. The PDF of $\sin^2\theta$ is derived as (see Appendix B)

$$f_{\sin^2\theta}(x)=\frac{1}{\pi\sqrt{x\,(1-x)}}. \tag{23}$$

Therefore, using [24, eq. (6-42)] and given that γ_{SR} is exponentially distributed with average value equal to $\overline{\gamma}_{SR}$, the PDF of SNR_{MIC} is derived from (22), (6) and (23) as

$$\begin{aligned}f_{SNR_{MIC}}(x)&=\int_0^1\frac{\exp\left(-\frac{x}{y\overline{\gamma}_{SR}}\right)}{\pi\overline{\gamma}_{SR}y\sqrt{y\,(1-y)}}dy\\&=\frac{\exp\left(-\frac{x}{\overline{\gamma}_{SR}}\right)}{\sqrt{x}\sqrt{\pi\overline{\gamma}_{SR}}}.\end{aligned} \tag{24}$$

Then, the CDF of SNR_{MIC} is derived using [20, eq. (3.361.1)] as

$$F_{SNR_{MIC}}(x)=\int_0^x f_{SNR_{MIC}}(y)\,dy=\text{erf}\left(\sqrt{\frac{x}{\overline{\gamma}_{SR}}}\right) \tag{25}$$

where $\text{erf}(\cdot)$ denotes the well-known error function.

Therefore, the occurrence probabilities of the cases $\Theta_1,...,\Theta_4$, as analyzed in Sections IV-A1-IV-A4, are derived as follows.

$$\rho_1=\text{erf}^2\left(\sqrt{\frac{T}{\overline{\gamma}_{SR}}}\right) \tag{26a}$$

$$\rho_2=\rho_3=\text{erf}\left(\sqrt{\frac{T}{\overline{\gamma}_{SR}}}\right)\text{erfc}\left(\sqrt{\frac{T}{\overline{\gamma}_{SR}}}\right) \tag{26b}$$

$$\rho_4=\text{erfc}^2\left(\sqrt{\frac{T}{\overline{\gamma}_{SR}}}\right) \tag{26c}$$

B. MGF and PDF of the Overall SINR, γ

Variation 2 leads to exactly the same expressions for the MGF and the PDF of γ as that of variation 1, yet with different occurrence probabilities regarding the cases $\Theta_1,...,\Theta_4$. Therefore, the MGF of γ for variation 2 is given by (19), by substituting $\rho_1,...,\rho_4$ with the corresponding expressions provided in (26); the PDF of γ is derived by plugging (26) into (21).

VI. Capacity and Outage Analysis

A. Average Capacity

The average capacity (per unit bandwidth) C_{av} of the proposed scheme can be written as

$$C_{av}=\int_0^\infty\log_2(1+\gamma)\,f_\gamma(\gamma)\,d\gamma. \tag{27}$$

Hence, we may obtain an approximate closed-form expression for C_{av} by plugging (21) in (27) yielding

$$\begin{aligned}C_{av}\simeq\rho_1&\Bigg[\Xi_1\mathcal{I}\left(\frac{L\overline{\gamma}_{RD}+1}{\overline{\gamma}_{SD}},0\right)+\sum_{i=2}^{L}\frac{\Xi_i\mathcal{I}\left(\frac{1}{\overline{\gamma}_{SD}},i-2\right)}{(i-2)!}\\&+\Psi_1\mathcal{I}\left(\frac{L\overline{\gamma}_{SD}+1}{\overline{\gamma}_{RD}},0\right)+\sum_{i=2}^{L}\frac{\Psi_i\mathcal{I}\left(\frac{1}{\overline{\gamma}_{RD}},i-2\right)}{(i-2)!}\Bigg]\\&+\rho_2\Bigg[\Delta_1\mathcal{I}\left(\frac{L\overline{\gamma}_{RD}+1}{\overline{\gamma}_{SD}},0\right)+\sum_{i=2}^{L}\frac{\Delta_i\mathcal{I}\left(\frac{1}{\overline{\gamma}_{SD}},i-2\right)}{(i-2)!}\Bigg]\\&+\rho_3\Bigg[\digamma_1\mathcal{I}\left(\frac{L\overline{\gamma}_{SD}+1}{\overline{\gamma}_{RD}},0\right)+\sum_{i=2}^{L}\frac{\digamma_i\mathcal{I}\left(\frac{1}{\overline{\gamma}_{RD}},i-2\right)}{(i-2)!}\\&+\sum_{i=1}^{L}\frac{\Upsilon_i\mathcal{I}\left(\frac{1}{\overline{\gamma}_{SD}},i-1\right)}{(i-1)!}\Bigg]+\rho_4\frac{\mathcal{I}\left(\frac{1}{\overline{\gamma}_{SD}},L-1\right)}{\overline{\gamma}_{SD}^{L}\,(L-1)!}.\end{aligned} \tag{28}$$

The auxiliary function $\mathcal{I}(\cdot,\cdot)$ used in (28) is defined as (please refer to Appendix C)

$$\begin{aligned}\mathcal{I}(b,m)&=\int_0^\infty x^m\log_2(1+x)\exp(-bx)\,dx\\&=\sum_{k=0}^{m}\frac{\binom{m}{k}e^b b^{k-m-1}}{(-1)^{k+1}\ln 2}\left[\Gamma(m-k+1)\left(\ln b-\psi(m-k+1)\right)\right.\\&\left.-\frac{{}_2F_2(1-k+m,1-k+m;2-k+m,2-k+m;-b)}{b^{k-m-1}\,(m-k+1)^2}\right]\end{aligned} \tag{29}$$

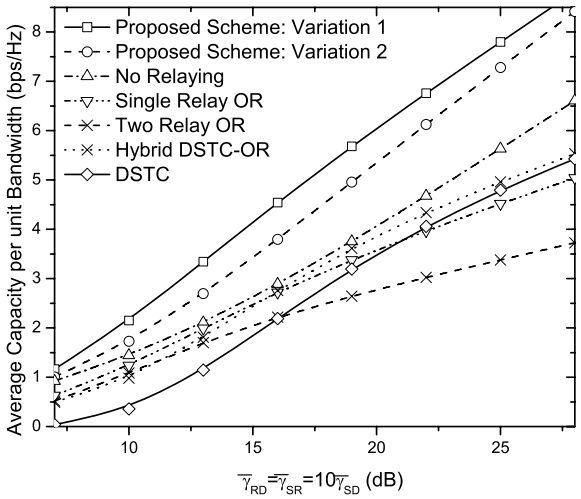

Fig. 3. Average capacity of the proposed scheme, as compared to orthogonal relaying (OR) with a single or two relays, the hybrid DSTC-OR, the DSTC and the no-relaying case, for $L = 2$ and $T = 10dB$.

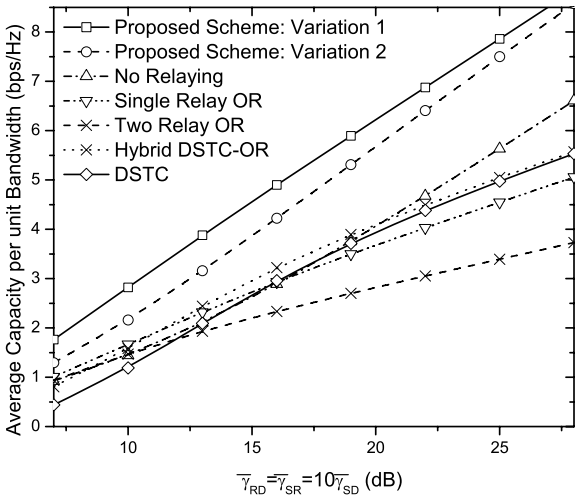

Fig. 4. Average capacity of the proposed scheme, as compared to orthogonal relaying (OR) with a single or two relays, the hybrid DSTC-OR, the DSTC and the no-relaying case, for $L = 2$ and $T = 6dB$.

where ${}_pF_q\left(\alpha_1, ..., \alpha_p; \beta_1, ..., \beta_q; z\right)$ and $\psi\left(\cdot\right)$ denotes the generalized hypergeometric function and the digamma function, defined in [20, eq. (9.141)] and [20, eq. (8.360.1)], respectively.

B. Outage Probability

The outage probability of the proposed scheme is actually the cumulative distribution function (CDF) of γ, evaluated at the outage threshold SNR γ_{th}, that is related to the target rate r through $\gamma_{th} = 2^r - 1$. Consequently, using (21), [20, eq. (3.381.3)] and [20, eq. (3.381.4)], we may derive an approximate closed-form expression for the outage probability as shown in (30) at the top of the next page. where $\Gamma\left(\cdot, \cdot\right)$ is the incomplete Gamma function defined in [20, eq. (8.350.2)].

VII. Numerical Examples and Discussion

The average capacity and outage performance of the proposed model are illustrated in Figs. 3-8, where the corresponding performances of five different schemes are also depicted, for comparison purposes. These schemes are a) classical point-to-point communications where no relaying takes place, b) threshold-based DF relaying with a single relay, satisfying the half-duplex constraint, c) threshold-based orthogonal DF relaying with two relays transmitting in orthogonal channels, d) Alamouti-based Distributed Space-Time Coding (DSTC) with two relays [27], where an outage occurs in case any of the relays is inactive due to insufficient quality of the corresponding S-R link and e) Hybrid DSTC - Orthogonal Relaying (OR), where in case one of the relays is in outage the other relay is utilized in OR fashion. We note that the comparison with the latter scheme is included in order to present a more fair comparison with the DSTC concept, since in a more complicated system the destination may switch to receiving from the active relay in a typical OR fashion, in case the other relay is inactive due to the thresholding mechanism. The x-axis refers to the average channel conditions on the relay-destination channels, which are assumed identical with the source-relay ones for the sake of simplicity. Moreover, the direct S-D channel is assumed relatively shadowed with respect to the relaying ones, so that $\overline{\gamma}_{SD} = \overline{\gamma}_{SR}/10 = \overline{\gamma}_{RD}/10$. The reasoning behind this assumption lies in the fact that in cases where multiple receiving antennas are employed, space diversity can combat small-scale fading but not the large-scale one; generally and loosely speaking, this is the case where relaying transmissions are expected to be employed, so as to tackle both small-scale fading and shadowing.

Figs. 3-4 depict the average capacity per unit bandwidth of the proposed scheme and the five comparison schemes mentioned above, for the case of $L = 2$ and $T = 10dB$, $T = 6dB$, respectively, presenting thus an outage comparison of the schemes under consideration, as well as the effect of the value of T on the outage performance. As can be seen from these Figs, variation 1 is superior than variation 2 in terms of average capacity, since the SNR at the relays is larger for variation 1, hence the relays' activation probabilities are also larger. As expected, the spectral efficiency advantage that the proposed model offers leads to generally higher capacity than that of OR, which becomes more evident in the high SNR regime. This is because of the orthogonality assumption that leads to a capacity decrease by a factor of $M+1$, where M is the total number of participating relays, resulting in a capacity expression that has the form of [3]

$$C_{CR} = \frac{1}{M+1}\log_2\left(1 + SNR\right) \tag{31}$$

where SNR is the instantaneous output SNR. In other words, one may conclude that the advantage of OR (that is, not to induce any interference) is contradicted by the spectral inefficiency that orthogonal transmissions entail, resulting in generally lower average capacity compared to that of the proposed scheme. Moreover, one may observe that the proposed scheme outperforms also the DSTC and Hybrid DSTC-OR schemes, which lead to a pre-log capacity decrease factor of $1/2$. Additionally, it is interesting to note that the proposed

$$P_o(\gamma_{th}) = \rho_1 \left[\frac{\Xi_1 \overline{\gamma}_{SD}}{L\overline{\gamma}_{RD}+1} \left(1 - e^{-\frac{L\overline{\gamma}_{RD}+1}{\overline{\gamma}_{SD}}\gamma_{th}}\right) + \sum_{i=2}^{L} \Xi_i \overline{\gamma}_{SD}^{i-1} \left(1 - \frac{\Gamma\left(i-1, \frac{\gamma_{th}}{\overline{\gamma}_{SD}}\right)}{\Gamma(i-1)}\right) + \frac{\Psi_1 \overline{\gamma}_{RD}}{L\overline{\gamma}_{SD}+1} \left(1 - e^{-\frac{L\overline{\gamma}_{SD}+1}{\overline{\gamma}_{RD}}\gamma_{th}}\right) \right.$$
$$\left. + \sum_{i=2}^{L} \Psi_i \overline{\gamma}_{RD}^{i-1} \left(1 - \frac{\Gamma\left(i-1, \frac{\gamma_{th}}{\overline{\gamma}_{RD}}\right)}{\Gamma(i-1)}\right) \right] + \rho_2 \left[\frac{\Delta_1 \overline{\gamma}_{SD}}{L\overline{\gamma}_{RD}+1} \left(1 - e^{-\frac{L\overline{\gamma}_{RD}+1}{\overline{\gamma}_{SD}}\gamma_{th}}\right) + \sum_{i=2}^{L} \Delta_i \overline{\gamma}_{SD}^{i-1} \left(1 - \frac{\Gamma\left(i-1, \frac{\gamma_{th}}{\overline{\gamma}_{SD}}\right)}{\Gamma(i-1)}\right) \right]$$
$$+ \rho_3 \left[\frac{\Gamma_1 \overline{\gamma}_{RD}}{L\overline{\gamma}_{SD}+1} \left(1 - e^{-\frac{L\overline{\gamma}_{SD}+1}{\overline{\gamma}_{RD}}\gamma_{th}}\right) + \sum_{i=2}^{L} \Gamma_i \overline{\gamma}_{RD}^{i-1} \left(1 - \frac{\Gamma\left(i-1, \frac{\gamma_{th}}{\overline{\gamma}_{RD}}\right)}{\Gamma(i-1)}\right) + \sum_{i=1}^{L} \Upsilon_i \overline{\gamma}_{SD}^{i} \left(1 - \frac{\Gamma\left(i, \frac{\gamma_{th}}{\overline{\gamma}_{SD}}\right)}{\Gamma(i)}\right) \right]$$
$$+ \rho_4 \left(1 - \frac{\Gamma\left(L, \frac{\gamma_{th}}{\overline{\gamma}_{SD}}\right)}{\Gamma(L)}\right) \tag{30}$$

model's superiority in terms of capacity is greater for high SNRs, owing to the concavity of the $\log(\cdot)$ function. Similar conclusions are obtained from Figs. 5-6, where five receiving antennas at the destination terminal are assumed and the relays activation threshold on the received SNR is again set to $T = 10dB$ and $T = 6dB$, respectively. Nevertheless, one may notice that the $L = 5$ case leads to greater capacity difference between the proposed model and the aforementioned comparison schemes. Hence, despite the fact that increasing L increases the diversity order in OR, DSTC and Hybrid DSTC-OR schemes, it seems that the proposed model takes better advantage of the large number of receiving antennas at the destination since in that case the spatial separation between the desired and the interfering signals through SDMA is more clearly distinguishable [15, Ch. 14].

Figs. 7-8 illustrate the outage performance of the proposed and the five comparison schemes, for the cases of target data rate $r = 1$bps/Hz and $r = 2$bps/Hz, respectively. In those Figs., the relay activation threshold, T, was set equal to the outage one, i.e., $T = 2^r - 1$ for the proposed scheme; $T = 2^{(M+1)r} - 1$ for OR, DSTC and Hybrid DSTC-OR, so as to follow the outage definition of relaying channels where an outage occurs if either the S-R or the R-D channels cannot support the desired spectral efficiency. The reader may also notice the tightness of the outage probability approximation shown in (30) as compared to simulation results, where the same assumptions regarding the outage, as well as the relay activation threshold were made.

As a general comment, one may notice that variation 1 offers improved outage performance, within the region of practical outage probabilities. Variation 2 on the other hand yields inferior outage performance, owing to the lower probabilities of activating the relays. Moreover, it is important to note that for high spectral efficiency requirements (for instance, in high data rate applications) the difference on the outage probability between the proposed and the OR systems increases. This is due to the aforementioned orthogonality assumption, that leads to an outage threshold SNR that has the form of

$$SNR_{th,CR} = 2^{(M+1)r} - 1 \tag{32}$$

i.e., higher than the proposed model's threshold SINR $\gamma_{th} = 2^r - 1$, which is the same as the SNR threshold of point-to-point communications. This implies that the beneficial effects of diversity that OR offers seem insufficient to support high spectral efficiencies without a large SNR increase, resulting in higher outage probabilities of OR, as compared to the proposed model. On the other hand, one may note that for low data rate requirements the outage probability of Hybrid DSTC-OR may be lower than that of the proposed scheme, particularly in the high SNR region. Generally speaking, one may conclude that the proposed scheme allows for reducing the transmitting power needed to achieve a given target rate, owing to the somewhat non-orthogonal setup. However, in the high SNR region the OR setup may still perform adequately.

VIII. Conclusions

In this paper we developed a relaying scheme that attains the beneficial effects of diversity without incurring any reduction in the overall spectral efficiency. This scheme takes advantage of the (extra) spatial dimension that multiple receiving antennas entail, so as to avoid orthogonal transmissions in either the time or frequency domain, keeping thus the overall spectral efficiency identical with that of communications under the conventional setup, where no relaying takes place. The analysis demonstrated that the proposed model outperforms orthogonal relaying and distributed space-time in terms of average capacity, as well as outage probability, due to its advantage of achieving high data rates without a large SNR sacrifice; it also outperforms point-to-point communications in cases of deep shadowing between the source and the destination. As a result, the proposed scheme appears as a suitable method for providing diversity gain in relay-assisted applications with high data rate requirements.

Appendix A
Derivation of the Approximate PDF of γ

Expanding the expression for the $\mathcal{M}_{\gamma_b^{S,R}}(s)$ shown in (20) in partial fractions yields

$$\mathcal{M}_{\gamma_b^{S,R}}(s) \simeq \frac{\Delta_1}{s + (L\overline{\gamma}_{RD}+1)/\overline{\gamma}_{SD}} + \sum_{i=2}^{L} \frac{\Delta_i}{\left(s + 1/\overline{\gamma}_{SD}\right)^{i-1}} \tag{33}$$

where the nominators are derived as

$$\Delta_i = \begin{cases} \frac{L\overline{\gamma}_{RD}+1}{\overline{\gamma}_{SD}} \left(-\frac{1}{L\overline{\gamma}_{RD}}\right)^{L-1}, & i = 1 \\ \frac{(L\overline{\gamma}_{RD}+1)\overline{\gamma}_{SD}^{1-i}}{(L\overline{\gamma}_{RD})^{L+1-i}} (-1)^{L-i}, & i = 2, ..., L \end{cases}. \tag{34}$$

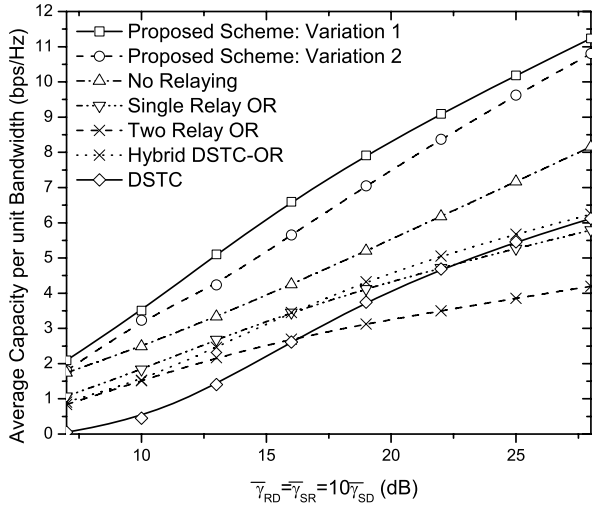

Fig. 5. Average capacity of the proposed scheme, as compared to orthogonal relaying (OR) with a single or two relays, the hybrid DSTC-OR, the DSTC and the no-relaying case, for $L = 5$ and $T = 10dB$.

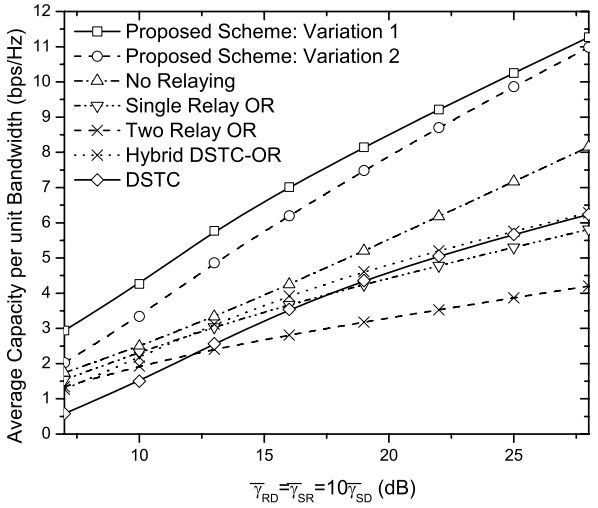

Fig. 6. Average capacity of the proposed scheme, as compared to orthogonal relaying (OR) with a single or two relays, the hybrid DSTC-OR, the DSTC and the no-relaying case, for $L = 5$ and $T = 6dB$.

Likewise, the MGF product $\mathcal{M}_{\gamma_b^{S,R}}(s)\,\mathcal{M}_{\gamma_b^{R,S}}(s)$ can be written as

$$\begin{aligned}&\mathcal{M}_{\gamma_b^{S,R}}(s)\,\mathcal{M}_{\gamma_b^{R,S}}(s)\\&\simeq\frac{\Xi_1}{s+\left(L\overline{\gamma}_{RD}+1\right)/\overline{\gamma}_{SD}}+\sum_{i=2}^{L}\frac{\Xi_i}{\left(s+1/\overline{\gamma}_{SD}\right)^{i-1}}\\&+\frac{\Psi_1}{s+\left(L\overline{\gamma}_{SD}+1\right)/\overline{\gamma}_{RD}}+\sum_{i=2}^{L}\frac{\Psi_i}{\left(s+1/\overline{\gamma}_{RD}\right)^{i-1}}\end{aligned}\tag{35}$$

where Ξ_i and Ψ_i are given in (36) and (37) shown at the top of the next page.

Working similarly, the product $\left(1+s\overline{\gamma}_{SD}\right)^{-L}\mathcal{M}_{\gamma_b^{R,S}}(s)$ is expanded in partial fractions as

$$\begin{aligned}&\left(1+s\overline{\gamma}_{SD}\right)^{-L}\mathcal{M}_{\gamma_b^{R,S}}(s)\simeq\frac{\digamma_1}{s+\left(L\overline{\gamma}_{SD}+1\right)/\overline{\gamma}_{RD}}\\&+\sum_{i=2}^{L}\frac{\digamma_i}{\left(s+1/\overline{\gamma}_{RD}\right)^{i-1}}+\sum_{i=1}^{L}\frac{\Upsilon_i}{\left(s+1/\overline{\gamma}_{SD}\right)^{i}}\end{aligned}\tag{39}$$

where Υ_i is given by

$$\begin{aligned}\Upsilon_i=&\frac{L\overline{\gamma}_{SD}+1}{(L-i)!\overline{\gamma}_{SD}^{L}\overline{\gamma}_{RD}^{L}}\\&\times\frac{\partial^{L-i}}{\partial s^{L-i}}\left[\frac{\left(1/\overline{\gamma}_{RD}+s\right)^{1-L}}{\left(L\overline{\gamma}_{SD}+1\right)/\overline{\gamma}_{RD}+s}\right]_{s=-\frac{1}{\overline{\gamma}_{SD}}}\end{aligned}\tag{40}$$

while $\digamma_i$ is shown in (38) at the top of the next page. The approximate PDF of γ is then derived by taking the inverse Laplace transform of the approximate MGF. Specifically, $f_\gamma(\cdot)$ can be evaluated in closed form by using (33)-(**??**) and the fact that $\mathcal{L}^{-1}\left\{(s+\alpha)^{-n}\right\}(x)=x^{n-1}\exp(-\alpha x)/(n-1)!$, where $\mathcal{L}^{-1}\{\cdot\}$ denotes the inverse Laplace transform operator, finally yielding (21).

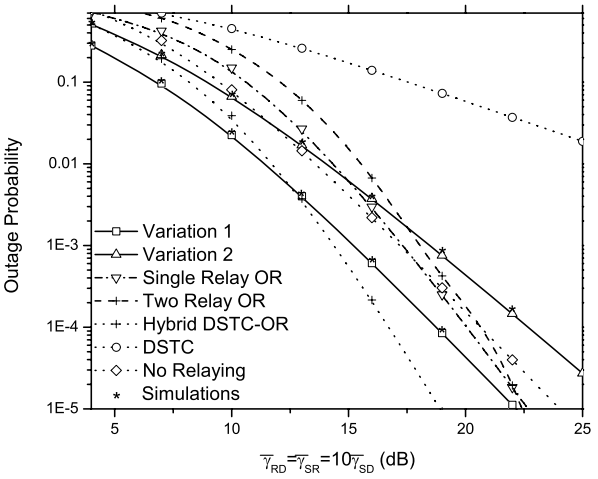

Fig. 7. Outage probability of the proposed scheme, as compared to orthogonal relaying (OR) with a single or two relays, the hybrid DSTC-OR, the DSTC and the no-relaying case, for $L = 3$ and $r = 1$.

APPENDIX B
DERIVATION OF THE CDF OF $\sin^2\theta$

Given that θ is uniformly distributed in $(-\pi,\pi]$, its PDF in this interval is given by $f_\theta(\theta)=1/2\pi$. Hence, the PDF of $\sin\theta$ is derived using the standard technique for transformation of a RV [24, eq. (5-5)], yielding

$$f_{\sin\theta}(x)=\frac{1}{\pi\cos\left(\arcsin(x)\right)}=\frac{1}{\pi\sqrt{1-x^2}}.\tag{41}$$

Then, using [24, eq. (5-8)], (41) yields (23).

$$\Xi_i = \begin{cases} -\frac{(L\overline{\gamma}_{RD}+1)(L\overline{\gamma}_{SD}+1)\overline{\gamma}_{SD}^{L-1}(L\overline{\gamma}_{SD}+L\overline{\gamma}_{RD}+1)^{-1}}{L^{L-1}(\overline{\gamma}_{RD}-\overline{\gamma}_{SD})\overline{\gamma}_{RD}^{L-1}\left(\overline{\gamma}_{RD}-\overline{\gamma}_{SD}+L\overline{\gamma}_{RD}^2\right)^{L-1}}, & i=1 \\ \frac{(L\overline{\gamma}_{RD}+1)(L\overline{\gamma}_{SD}+1)}{(L-i)!\overline{\gamma}_{SD}^{L}\overline{\gamma}_{RD}}\frac{\partial^{L-i}}{\partial s^{L-i}}\left[\frac{(1+\overline{\gamma}_{RD}s)^{1-L}}{[(L\overline{\gamma}_{RD}+1)/\overline{\gamma}_{SD}+s][(L\overline{\gamma}_{SD}+1)/\overline{\gamma}_{RD}+s]}\right]_{s=-\frac{1}{\overline{\gamma}_{SD}}}, & i=2,...,L \end{cases} \tag{36}$$

$$\Psi_i = \begin{cases} -\frac{(L\overline{\gamma}_{SD}+1)(L\overline{\gamma}_{RD}+1)\overline{\gamma}_{RD}^{L-1}(L\overline{\gamma}_{RD}+L\overline{\gamma}_{SD}+1)^{-1}}{L^{L-1}(\overline{\gamma}_{SD}-\overline{\gamma}_{RD})\overline{\gamma}_{SD}^{L-1}\left(\overline{\gamma}_{SD}-\overline{\gamma}_{RD}+L\overline{\gamma}_{SD}^2\right)^{L-1}}, & i=1 \\ \frac{(L\overline{\gamma}_{SD}+1)(L\overline{\gamma}_{RD}+1)}{(L-i)!\overline{\gamma}_{RD}^{L}\overline{\gamma}_{SD}}\frac{\partial^{L-i}}{\partial s^{L-i}}\left[\frac{(1+\overline{\gamma}_{SD}s)^{1-L}}{[(L\overline{\gamma}_{SD}+1)/\overline{\gamma}_{RD}+s][(L\overline{\gamma}_{RD}+1)/\overline{\gamma}_{SD}+s]}\right]_{s=-\frac{1}{\overline{\gamma}_{RD}}}, & i=2,...,L \end{cases}. \tag{37}$$

$$F_i = \begin{cases} \frac{\overline{\gamma}_{RD}^{L-1}(L\overline{\gamma}_{SD}+1)}{\overline{\gamma}_{SD}^{L-1}L^{L-1}[\overline{\gamma}_{RD}-\overline{\gamma}_{SD}(L\overline{\gamma}_{SD}+1)]^{L}}\left(-1\right)^{L-1}, & i=1 \\ \frac{L\overline{\gamma}_{SD}+1}{(L-i)!\overline{\gamma}_{SD}^{L}\overline{\gamma}_{RD}^{L}}\frac{\partial^{L-i}}{\partial s^{L-i}}\left[\frac{(1/\overline{\gamma}_{SD}+s)^{-L}}{(L\overline{\gamma}_{SD}+1)/\overline{\gamma}_{RD}+s}\right]_{s=-\frac{1}{\overline{\gamma}_{RD}}}, & i=2,...,L \end{cases} \tag{38}$$

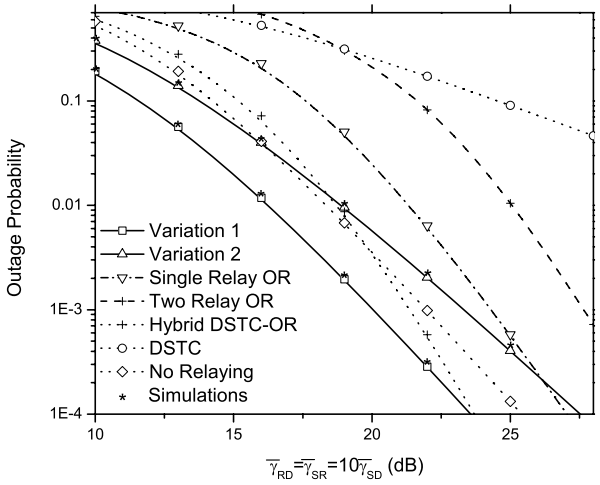

Fig. 8. Outage probability of the proposed scheme, as compared to orthogonal relaying (OR) with a single or two relays, the hybrid DSTC-OR, the DSTC and the no-relaying case, for $L=3$ and $r=2$.

APPENDIX C
DERIVATION OF $\mathcal{I}(\cdot,\cdot)$

Using the variable change $y=x+1$, the auxiliary function $\mathcal{I}(b,m)$ can be written as

$$\begin{aligned} \mathcal{I}(b,m) &= \int_1^{\infty}(y-1)^m\frac{\ln(y)}{\ln 2}\exp\left(-b(y-1)\right)dy \\ &= \sum_{k=0}^{m}\binom{m}{k}\frac{(-1)^k}{\ln 2}\int_1^{\infty}y^{m-k}\ln(y)\exp\left(-b(y-1)\right)dy. \end{aligned} \tag{42}$$

where the last equation is derived by expanding $(y-1)^m$ into binomial series. Then, (29) is inferred from (42) after some manipulations, using [20, eq. (4.358.1)], the definition of $\psi(\cdot)$ [20, eq. (8.360.1)] and the infinite series representation of $\Gamma(\cdot,\cdot)$ and ${}_2F_2(\cdot,\cdot;\cdot,\cdot;\cdot)$ given in [20, eq. (8.354.2)] and [20, eq. (9.14.1)], respectively.

ACKNOWLEDGMENT

The authors would like to thank Mr. Athanasios S. Lioumpas for conducting the simulations.

REFERENCES

[1] J. N. Laneman, D. N. C. Tse, and G. W. Wornell, "Cooperative diversity in wireless networks: efficient protocols and outage behavior," *IEEE Trans. Inf. Theory*, vol. 50, pp. 3062-3080, Dec. 2004.

[2] I. Maric and R. Yates, "Forwarding strategies for Gaussian parallel-relay networks," in *Proc. Conf. Inf. Sciences Syst. CISS 2004*, Princeton, NJ, Mar. 2004.

[3] N. C. Beaulieu and J. Hu, "A closed-form expression for the outage probability of decode-and-forward relaying in dissimilar Rayleigh fading channels," *IEEE Commun. Lett.*, vol. 10, pp. 813-815, Dec. 2006.

[4] Y. Zhao, R. Adve, and T. J. Lim, "Outage probability at arbitrary SNR with cooperative diversity," *IEEE Commun. Lett.*, vol. 9, pp. 700-702, Aug. 2005.

[5] ——, "Improving amplify-and-forward relay networks: optimal power allocation versus selection," in *Proc. IEEE Intern. Symp. Inf. Theory (ISIT 06)*, Seattle, WA, July 2006.

[6] H. Mheidat and M. Uysal, "Impact of receive diversity on the performance of amplify-and-forward relaying under APS and IPS power constraints," *IEEE Commun. Lett.*, vol. 10, pp. 468-470, June 2006.

[7] M. Safari, M. Uysal, and K. Zhang, "Cooperative diversity over log-normal fading channels: performance analysis and optimization," *IEEE Trans. Wireless Commun.*, accepted for publication.

[8] Y. Zhao, R. Adve, and T. J. Lim, "Symbol error rate of selection amplify-and-forward relay systems," *IEEE Commun. Lett.*, vol. 10, pp. 757-759, Nov. 2006.

[9] S. Ikki and M. H. Ahmed, "Performance analysis of cooperative diversity wireless networks over Nakagami-m fading channel," *IEEE Commun. Lett.*, vol. 11, pp. 334-336, Apr. 2007.

[10] P. A. Anghel and M. Kaveh, "Exact symbol error probability of a cooperative network in a Rayleigh-fading environment," *IEEE Trans. Wireless Commun.*, vol. 3, pp. 1416-1421, Sep. 2004.

[11] A. Ribeiro, X. Cai, and G. Giannakis, "Symbol error probabilities for general cooperative links," *IEEE Trans. Wireless Commun.*, vol. 4, pp. 1264-1273, May 2005.

[12] B. Rankov and A. Wittneben, "Spectral efficient protocols for half-duplex fading relay channels," *IEEE J. Sel. Areas Commun.*, vol. 25, pp. 379-389, Feb. 2007.

[13] H. S. Ryu, C. G. Kang, and D. S. Kwon, "Transmission protocol for cooperative MIMO with full rate: design and analysis," in *Proc. Veh. Technol. Conf. (VTC Spring'07)*, Dublin, Ireland, 2007.

[14] Y. Fan, C. Wang, J. Thompson, and H. V. Poor, "Recovering multiplexing loss through successive relaying using repetition coding," *IEEE Trans. Wireless Commun.*, vol. 6, pp. 4484-4493, Dec. 2007.

[15] A. Goldsmith, *Wireless Communications*, 1st edition. Cambridge, UK: Cambridge University press, 2005.

[16] D. Tse and P. Viswanath, *Fundamentals of Wireless Communication*, 1st edition. Cambridge, UK: Cambridge University press, 2005.

[17] W. P. Siriwongpairat, T. Himsoon, W. Su, and K. J. R. Liu, "Optimum threshold-selection relaying for decode-and-forward cooperation protocol," in *Proc. IEEE Wireless Commun. Netw. Conf. (WCNC'06)*, Las Vegas, NV, USA, Apr. 2006.

[18] R. Meyer, W. H. Gerstacker, R. Schober, and J. B. Huber, "A single antenna interference cancellation algorithm for increased GSM capacity," *IEEE Trans. Wireless Commun.*, vol. 5, pp. 1616-1621, July 2006.

[19] J. H. Winters, "Optimum combining in digital mobile radio with cochannel interference," *IEEE J. Sel. Areas Commun.*, vol. 2, pp. 528-539, July 1984.

[20] I. S. Gradshteyn and I. M. Ryzhik, *Table of Integrals, Series, and Products*, 6th edition. New York: Academic, 2000.

[21] R. K. Mallik, M. Z. Win, M. Chiani, and A. Zanella, "Bit-error probability for optimum combining of binary signals in the presence of interference and noise," *IEEE Trans. Wireless Commun.*, vol. 3, pp. 395-407, Mar. 2004.

[22] V. A. Aalo and J. Zhang, "Performance of antenna array systems with optimum combining in a Rayleigh fading environment," *IEEE Commun. Lett.*, vol. 4, pp. 125-127, Apr. 2000.

[23] M. Abramovitz and I. A. Stegun, *Handbook of Mathematical Functions with Formulas, Graphs, and Mathematical Tables*, 9th edition. New York: Dover, 1972.

[24] A. Papoulis, *Probability, Random Variables, and Stochastic Procceses*, 3rd edition. McGraw-Hill, 1991.

[25] T. D. Pham and K. G. Balmain, "Multipath performance of adaptive antennas with multiple interferers and correlated fadings," *IEEE Trans. Veh. Technol.*, vol. 48, pp. 342-352, Mar. 1999.

[26] M. Konrad and W. Gerstacker, "Interference robust transmission for the downlink of an OFDM-based mobile communications system," *EURASIP J. Wireless Commun. Netw.*, vol. 2008, article ID = 549371, 14 pages.

[27] P. A. Anghel, G. Leus, and M. Kaveh, "Distributed space-time cooperative systems with regenerative relays," *IEEE Trans. Wireless Commun.*, vol. 5, pp. 3130-3141, Nov. 2006.

Diomidis S. Michalopoulos (S'05, M'10) was born in Thessaloniki, Greece, in 1983. He received the Diploma of Electrical and Computer Engineering in July 2005, from the Aristotle University of Thessaloniki. In September 2005 he joined the wireless communications systems group (WCSG); he obtained a Ph.D. degree from the ECE department in May 2009. Since September 2009, he is with the University of British Columbia, Vancouver, Canada, as a Killam postdoctoral fellow. His research interests span in the areas of physical layer analysis of Wireless Multihop and Cooperative Systems and wireless Free Space Optical Communications. Dr. Michalopoulos is co-recipient of the Best Paper Award of the Wireless Communications Symposium (WCS) in IEEE International Conference on Communications (ICC'07).

George K. Karagiannidis (M'97-SM'04) was born in Pithagorion, Samos Island, Greece. He received the University Diploma (5 years) and Ph.D degree, both in electrical and computer engineering from the University of Patras, in 1987 and 1999, respectively.

From 2000 to 2004, he was a Senior Researcher at the Institute for Space Applications and Remote Sensing, National Observatory of Athens, Greece. In June 2004, he joined Aristotle University of Thessaloniki, Thessaloniki, where he is currently an Associate Professor of Digital Communications Systems in the Electrical and Computer Engineering Department and Head of the Telecommunications Systems and Networks Lab. His current research interests are in the broad area of digital communications systems with emphasis on cooperative communication, adaptive modulation, MIMO, optical wireless and underwater communications.

He is the author or co-author of more than 110 technical papers published in scientific journals and presented at international conferences. He is also a co-author of three chapters in books and author of the Greek edition of a book on Telecommunications Systems. Dr. Karagiannidis has been a member of Technical Program Committees for several IEEE conferences as ICC, GLOBECOM, etc. He is a member of the editorial boards of the IEEE TRANSACTIONS ON COMMUNICATIONS, IEEE COMMUNICATIONS LETTERS and Lead Guest Editor of the special issue on "Optical Wireless Communications" of the IEEE JOURNAL ON SELECTED AREAS IN COMMUNICATIONS.

He is co-recipient of the Best Paper Award of the Wireless Communications Symposium (WCS) in IEEE International Conference on Communications (ICC'07), Glasgow, U.K., June 2007. Dr. Karagiannidis is the Chair of the IEEE COMSOC Greek Chapter.